

Valeria Ferrari^{(1)*}, Massimo Pauri^{(2)†} and Federico Piazza^{(3)‡}⁽¹⁾*Dipartimento di Fisica, Università di Roma, “La Sapienza” and**I.N.F.N. Sezione di Roma1, Piazzale Aldo Moro 5, Roma, Italy*⁽²⁾*Dipartimento di Fisica, Università di Parma and**I.N.F.N. Gruppo Collegato di Parma, Viale delle Scienze, 43100, Parma, Italy*⁽³⁾*Dipartimento di Fisica, Università di Milano and I.N.F.N. Sezione di Milano, Via Celoria 16, 20133 Milano, Italy*

(Received 30 May 2000)

In this paper we study the perturbations of the charged, dilaton black hole, described by the solution of the low energy limit of the superstring action found by Garfinkle, Horowitz and Strominger. We compute the complex frequencies of the quasi-normal modes of this black hole, and compare the results with those obtained for a Reissner-Nordström and a Schwarzschild black hole. The most remarkable feature which emerges from this study is that the presence of the dilaton breaks the *isospectrality* of axial and polar perturbations, which characterizes both Schwarzschild and Reissner-Nordström black holes.

PACS numbers: 04.30.Db, 04.70.Bw, 04.40.Nr

I. INTRODUCTION

The study of the effects produced by the coupling between gravity and scalar fields is a rather hot issue, since a definite prediction of superstring theory is just the existence of a scalar field, namely the *dilaton*. For instance, this coupling could have played an important role during the early phases of the life of the Universe. Indeed, it has been shown that a possible cosmological implication of the dilaton is the so-called “pre-big-bang” scenario [2], characterized by a dilaton-driven inflationary period, that should have left its peculiar fingerprints on the cosmic gravitational wave background [3]. On the experimental side, recent investigations on the interaction of scalar waves with gravitational detectors have shown that a scalar component of the gravitational radiation should excite the monopole mode of a resonant spherical antenna [4] and also give rise to specific correlations between the signals revealed by a resonant sphere and an interferometer [5].

Among all possible astrophysical sources of gravitational waves, black holes should have the most typical and in principle recognizable frequency spectrum. According to the Einstein theory of gravity, a black hole which dynamically interacts with its surroundings emits wave bursts having shape and intensity which initially depend on the features of the external perturbations. As a late-time effect, however, it generates gravitational wave trains having characteristic frequencies which are *independent* of the initial perturbations, the so-called *quasi normal modes* [6]. And we know from the theory that these frequencies can only depend on the three parameters characterizing a black hole, namely the mass, the charge and the angular momentum.

The question whether a black hole can support an additional scalar degree of freedom and still generate a regular, asymptotically flat, spacetime free of naked singularities or any other kind of pathological behaviour has been widely investigated in the literature. Having in mind the “no-hair theorem” program, Bekenstein [7] in 1972 showed that black holes cannot support a *minimally coupled* scalar field, if the solution is required to be asymptotically flat. Subsequently, he developed a procedure to generate black hole solutions surrounded by a *conformal* scalar field [8], but they proved to be *unstable* against radial perturbations [9]. In 1990 Ferrari and Xanthopoulos [10], using a Kaluza-Klein approach, derived equations describing a gravitational field coupled with a massive scalar field, obtained the conformal structure of the metric, and discussed several kind of possible couplings. Yet, no definite answer was given to the question whether a satisfactory black hole can exist surrounded by a massive scalar field.

The search for regular exact solutions describing black holes endowed with a scalar field got a formidable boost when it became clear that, as long as the curvature is small, all vacuum solutions of general relativity are also approximate

*Email address: Valeria.Ferrari@roma1.infn.it

†Email address: pauri@pr.infn.it

‡Email address: piazza@mi.infn.it

solutions of string theory. As a matter of fact, charged black hole solutions coupled to a scalar field, viz a *dilaton* in this context, can be obtained by the action (we use geometric units throughout)

$$S = \int d^4x \sqrt{-g} [R - 2(\nabla\phi)^2 + e^{-2a\phi} F^2], \quad (1)$$

which, by variations, gives the equations:

$$\nabla_\mu (e^{-2a\phi} F^{\mu\nu}) = 0, \quad (2)$$

$$\nabla^2\phi - \frac{1}{2}e^{-2a\phi} F^2 = 0, \quad (3)$$

$$R_{\mu\nu} = 2\nabla_\mu\phi\nabla_\nu\phi - 2e^{-2a\phi}F_{\mu\rho}F_\nu{}^\rho + \frac{1}{2}g_{\mu\nu}e^{-2a\phi}F^2, \quad (4)$$

where $F^2 = F_{\mu\nu}F^{\mu\nu}$ is the first Maxwell invariant and a is a non-negative real constant regulating the strength of the coupling between the dilaton and the Maxwell field. This theory has a number of interesting limiting cases. The limit $a = 0$ corresponds to the ordinary Einstein-Maxwell theory plus a Klein-Gordon scalar field with zero mass. The case $a = \sqrt{3}$ is the four-dimensional reduction of Kaluza-Klein theory. Finally, for $a = 1$ the action (1) describes the tree-level low energy limit of superstring theory in the so-called *Einstein frame*. A large class of black hole solutions of this theory in an arbitrary number of dimensions has been found by Gibbons and Maeda [11]. Their results were next specialized to four dimensions by Garfinkle, Horowitz and Strominger [1] (GHS) who studied a solution describing a spherically symmetric, charged, dilaton black hole. In the GHS solution the electric charge and the dilaton are not independent parameters: when the charge is set equal to zero the dilaton also disappears, and the solution reduces to that of a Schwarzschild black hole. In a sense, this is a consequence of the “no-hair theorems” which limits the number of free parameters of a black hole to three.

The equations satisfied by small perturbations of this solution have been derived and studied by Holzhey and Wilczek [13] in the line of the general treatment given by Chandrasekar [12]. They first showed that it is possible to reduce the perturbed equations to five decoupled wave equations with potential barriers, and, as a by-product of their analysis, they argued that the GHS solution is stable under external small perturbations.

In this paper we take a further step in the study the properties of the coupled emission of electromagnetic, scalar and gravitational radiation by such black holes, computing the *quasi-normal mode frequencies* of the GHS solution. Comparing the spectrum of the latter with those of Schwarzschild and Reissner-Nordström, we show that the presence of the scalar field breaks the relevant feature of the *isospectrality* of the axial and polar perturbations.

The paper is organized as follows. In Section 2 we summarize the features of the GHS solution. In Sections 3 and 4 the equations governing the axial and polar perturbations are discussed separately. We shall not derive the axial equations, since there is nothing to add to the derivation made in Ref. [13]. On the other hand, the polar equations will be discussed in greater detail. Some misprints appearing in Ref. [13] are corrected and the explicit expression of the matrix whose eigenvalues are the potentials governing polar perturbations is given in the Appendix. In Section 5 the quasi-normal frequencies of the GHS black hole obtained with an extended WKB approach [16] are calculated for different values of the parameters. Finally, in Section 6 the results obtained are discussed and the main qualitative differences between the spectra of the dilaton and the Reissner Nordström black holes are pointed out.

II. THE EXACT SOLUTION

The exact solution of equations (2)-(4), with $a = 1$, describing the charged dilaton black hole we study in this paper is [1]

$$ds^2 = \left(1 - \frac{2M}{r}\right) dt^2 - \left(1 - \frac{2M}{r}\right)^{-1} dr^2 - r \left(r - \frac{Q_e^2}{M}\right) [d\theta^2 + \sin^2\theta d\varphi^2] \quad (5)$$

where M and Q_e are, respectively, the black hole mass and electric charge. $F_{tr} = Q_e/r^2$ is the only non-vanishing component of the electromagnetic tensor, and the scalar field is related to the electric charge by the following equation

$$e^{2\phi} = \left(1 - \frac{Q_e^2}{Mr}\right), \quad (6)$$

which shows that ϕ vanishes at radial infinity. Since the dilaton and the electric charge are coupled through Eq. (6), the Reissner Nördstrom solution cannot be obtained as a limiting case of the metric (5). On the other hand, the Schwarzschild solution is recovered from Eq. (5) by setting $Q_e = 0$.

It should be noted that the usual relation between radius and area of the spheres $t = \text{const}$, $r = \text{const}$ is obtained in terms of the modified radial variable

$$\tilde{r} = \sqrt{r \left(r - \frac{Q_e^2}{M} \right)},$$

and not of r , by the usual relation $A(r) = 4\pi\tilde{r}^2$.

The metric (5) appears to be singular in $r = 0$, $r = Q_e^2/M$ and $r = 2M$. The surface $r = 2M$ is an event horizon, whereas on $r = Q_e^2/M$ the curvature scalar

$$R = 2g^{rr}(\phi_{,r})^2 = \frac{1}{2} \left(1 - \frac{2M}{r} \right) \frac{Q_e^2}{r(Mr - Q_e^2)},$$

diverges, showing that there is a curvature singularity. In $r = Q_e^2/M$, the radial coordinate \tilde{r} vanishes and loses its meaning for $r < Q_e^2/M$. Thus, a physical observer who crosses the event horizon terminates its journey on the curvature singularity.

In order to avoid naked singularities, in what follows we shall assume that

$$2M^2 > Q_e^2.$$

As shown in Ref. [12] (to be referred to hereafter as MT), the study of the perturbations of the metric (5), can be restricted, without loss of generality, to axisymmetric perturbations only. The appropriate metric in this case is

$$ds^2 = e^{2\nu}(dt)^2 - e^{2\psi}(d\phi - q_2 dx^2 - q_3 dx^3 - \omega dt)^2 - e^{2\mu_2}(dx^2)^2 - e^{2\mu_3}(dx^3)^2, \quad (7)$$

where, in the unperturbed state,

$$\begin{aligned} e^{2\nu} &= e^{-2\mu_2} = \left(1 - \frac{2M}{r} \right), & e^{2\psi} &= \tilde{r}^2 \sin^2 \theta \\ e^{2\mu_3} &= \tilde{r}^2, & \omega &= q_2 = q_3 = 0, \end{aligned} \quad (8)$$

and $(0, 1, 2, 3)$ stand for $(t, \varphi, r, \vartheta)$. We shall assume that, as a consequence of a generic perturbation, the metric functions, the electromagnetic quantities and the scalar field will experience small changes with respect to their unperturbed values

$$\begin{aligned} \nu &\longrightarrow \nu + \delta\nu, & \mu_2 &\longrightarrow \mu_2 + \delta\mu_2, & \psi &\longrightarrow \psi + \delta\psi, \\ \mu_3 &\longrightarrow \mu_3 + \delta\mu_3, & \omega &\longrightarrow \delta\omega, & q_2 &\longrightarrow \delta q_2, \\ q_3 &\longrightarrow \delta q_3, & F_{\mu\nu} &\longrightarrow F_{\mu\nu} + \delta F_{\mu\nu}, & \phi &\longrightarrow \phi + \delta\phi. \end{aligned}$$

Since the perturbation is assumed to be axisymmetric, all perturbed quantities depend on t , r and θ only. As in MT, it is convenient to project Einstein's and Maxwell's equations onto an orthonormal tetrad frame, and assume that all perturbed functions have the time dependence $e^{i\sigma t}$. The separation of variables is accomplished by expanding all perturbed tensors in tensorial spherical harmonics. These harmonics belong to two different classes, depending on the way they behave under the angular transformation $\theta \rightarrow \pi - \theta$ and $\phi \rightarrow \pi + \phi$. Those that transform like $(-1)^{(\ell+1)}$ are termed *axial*, those that transform like $(-1)^\ell$ are termed *polar*. The perturbed equations split into two decoupled sets corresponding to a different parity.

III. THE AXIAL EQUATIONS

The axial equations for $\ell \geq 2$ are obtained by perturbing the $\{12\}$ and $\{13\}$ -components of the Einstein equations. The separation of variables, can be accomplished by putting

$$\tilde{r}^2 e^{2\nu} \sin^3 \theta [q_{2,3}(t, r, \vartheta) - q_{3,2}(t, r, \vartheta)] = Q_\ell(r, \sigma) C_{\ell+2}^{-3/2}(\vartheta) e^{i\sigma t},$$

and

$$F_{01}(t, r, \vartheta) \sin \vartheta = 3B_\ell(r, \sigma) C_{\ell+1}^{-1/2}(\vartheta) e^{i\sigma t},$$

where $C_{\ell+1}^{-1/2}(\vartheta)$ are the Gegenbauer polynomials. As shown in Ref. [13], the axial equations can be cast in the following form

$$\left(\frac{d^2}{dr_*^2} + \sigma^2 \right) \begin{pmatrix} H_{1\ell} \\ H_{2\ell} \end{pmatrix} = \mathbf{B} \begin{pmatrix} H_{1\ell} \\ H_{2\ell} \end{pmatrix} \quad (9)$$

where

$$\mathbf{B} = \frac{e^{2\nu}}{\tilde{r}^2} \left[\left(\mu^2 + 2 + \frac{Q_e^2}{r^2} + \frac{3Q_e^4}{4M^2\tilde{r}^2} e^{2\nu} \right) \begin{pmatrix} 1 & 0 \\ 0 & 1 \end{pmatrix} + \frac{1}{r} \begin{pmatrix} Q_e^2/M & 2\mu Q_e \\ 2\mu Q_e & -6M \end{pmatrix} \right], \quad (10)$$

r_* is the tortoise coordinate defined by the equation

$$dr_* = e^{-2\nu} dr, \quad (11)$$

and $\mu^2 = (\ell - 1)(\ell + 2)$. The radial functions H_1 and H_2 (from now on we omit the index ℓ) are related to the perturbed metric and electromagnetic functions by the following relations

$$Q(r, \sigma) = \tilde{r} H_2(r, \sigma) \quad re^\nu B(r, \sigma) = \frac{H_1(r, \sigma)}{2\mu}. \quad (12)$$

The right hand side of Eq. (9) can be obviously diagonalized by a linear r -independent transformation, in the form

$$\begin{aligned} Z_1^a &= \mathcal{L}_1 H_1 + \mathcal{L}_2 H_2, \\ Z_2^a &= \mathcal{L}_2 H_1 - \mathcal{L}_1 H_2, \end{aligned} \quad (13)$$

where

$$\mathcal{L}_1 = \frac{Q_e^2}{2M} + 3M + \sqrt{\frac{Q_e^4}{4M^2} + 9M^2 + Q_e^2(3 + 4\mu^2)} \quad \text{and} \quad \mathcal{L}_2 = 2\mu Q_e. \quad (14)$$

Then the system (9) decouples in two wave equations:

$$\left(\frac{d^2}{dr_*^2} + \sigma^2 \right) Z_i^a = V_i^a Z_i^a \quad (i = 1, 2), \quad (15)$$

where the explicit form of the effective potentials is

$$V_{1,2}^a = \frac{e^{2\nu}}{r\tilde{r}^2} \left[(\mu^2 + 2)r + \frac{Q_e^2}{r} + \frac{3Q_e^4 r}{4M^2\tilde{r}^2} e^{2\nu} + \frac{Q_e^2}{2M} - 3M \pm \sqrt{\frac{Q_e^4}{4M^2} + 9M^2 + Q_e^2(3 + 4\mu^2)} \right]. \quad (16)$$

Equation (14) shows that when Q_e vanishes, $\mathcal{L}_2 = 0$; in this case Z_2^a reduces to the gravitational perturbation and V_2^a to the Regge-Wheeler potential, whereas Z_1^a reduces to the pure electromagnetic perturbation of a Schwarzschild black hole, which is known to be independent of gravitational contributions. If the electromagnetic charge does not vanish, the gravitational and electromagnetic perturbations are coupled; a gravitational wave incident on the potential barriers induces the emission of electromagnetic radiation and viceversa. On the other hand, the dilaton is not dynamically coupled with the axial perturbations. Its effect is that of shaping the effective potentials together with the electric field. In a similar manner, the energy density and the pressure of the matter composing a perturbed star determine the potential barrier of the axial perturbations without being dynamically coupled to the perturbed gravitational field.

The $\ell = 2$ potentials V_1^a and V_2^a are plotted in Fig. ?? versus the rescaled tortoise coordinate r_*/M for different values of the electric charge. We see that they always tend to zero at radial infinity and at the black hole horizon, except when the charge assumes its extremal value $Q_e^2 = 2M^2$. In this case they take the form of a step, reflecting all waves whose square frequency is lower than their limiting value on the horizon.

We also see that for non extremal black holes the maximum of the barrier moves towards the horizon as the electric charge increases.

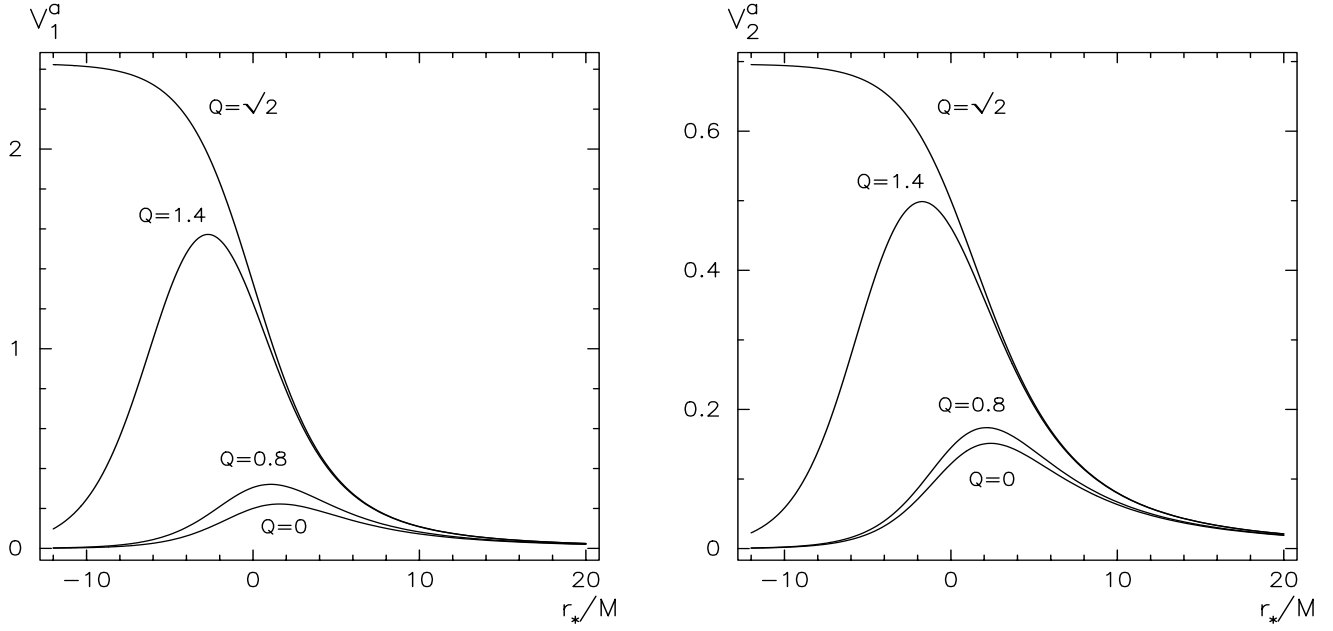


FIG. 1. The $\ell = 2$ axial potentials V_1^a (left) and V_2^a (right) are plotted versus the rescaled tortoise coordinate for different values of $Q = Q_e/M$. When the charge is set equal to zero, V_1^a reduces to that of the wave equation governing the pure electromagnetic perturbations of a Schwarzschild black hole, whereas V_2^a reduces to the Regge-Wheeler potential.

IV. THE POLAR EQUATIONS

The separation of variables for polar equations is accomplished by requiring that the perturbed functions have the angular dependence deriving from the expansion in tensor spherical harmonics:

$$\begin{aligned}
\delta\nu &= N_\ell(r)P_\ell(\theta)e^{i\sigma t}, \\
\delta\mu_2 &= L_\ell(r)P_\ell(\theta)e^{i\sigma t}, \\
\delta\psi &= [T_\ell(r)P_\ell(\theta) + 2\mu^{-2}X_\ell(r)P_{\ell,\theta}(\theta)\cot\theta]e^{i\sigma t}, \\
\delta\mu_3 &= [T_\ell(r)P_\ell(\theta) + 2\mu^{-2}X_\ell(r)P_{\ell,\theta,\theta}(\theta)]e^{i\sigma t}, \\
\delta F_{02} &= -\frac{e^{2\nu}\tilde{r}^2}{2Q_e}B_{02\ell}(r)P_\ell(\theta)e^{i\sigma t} \\
\delta F_{03} &= \frac{\tilde{r}}{2Q_e}B_{03\ell}(r)P_{\ell,\theta}(\theta)e^{i\sigma t}, \\
\delta F_{23} &= \frac{ie^{-\nu}\sigma\tilde{r}}{2Q_e}B_{23\ell}(r)P_{\ell,\theta}(\theta)e^{i\sigma t}, \\
\delta\phi &= \Phi P_\ell(\theta)e^{i\sigma t},
\end{aligned}$$

where $P_\ell(\theta)$ are the Legendre polynomials. In the following, we shall omit the index ℓ in all radial functions. Among the eight radial functions, N , L , T , X , B_{02} , B_{03} , B_{23} and Φ , the function T can be eliminated from the perturbed equations by making use of the relation that follows from the $\{03\}$ -component of the perturbed Einstein equations

$$B_{23} - T - L + 2\mu^{-2}X = 0. \quad (17)$$

From the polar components of the Maxwell's equations (see MT, Chap. 5 Eqs. (165)-(167) for the Reissner Nördstrom case), it is easy to derive a second order equation for B_{23} :

$$\left[\frac{\tilde{r}^2}{r^2} e^{2\nu} (r^2 B_{23})_{,r} \right]_{,r} + [\sigma^2 \tilde{r}^2 e^{-2\nu} - (\mu^2 + 2)] B_{23}$$

$$+\frac{2Q_e^2}{r^2}(2B_{23}-3L-2X-N-2\Phi)=0. \quad (18)$$

The Einstein equations for δR_{02} , δR_{23} , δG_{22} and δR_{11} give:

$$\left(\frac{d}{dr}+(\log \tilde{r}e^{-\nu})_{,r}\right)(B_{23}-L-X)-(\log \tilde{r})_{,r}L+\phi_{,r}\Phi=0, \quad (19)$$

$$(N-L)_{,r}-(\log \tilde{r}e^{\nu})_{,r}L-(\log \tilde{r}e^{-\nu})_{,r}N-\frac{2}{r}B_{23}+2\phi_{,r}\Phi=0, \quad (20)$$

$$X_{,r,r}+2(\log \tilde{r}e^{\nu})_{,r}X_{,r}+\frac{\mu^2e^{-2\nu}}{2\tilde{r}^2}(N+L)+\sigma^2e^{-4\nu}X=0, \quad (21)$$

$$\begin{aligned} &2(\log \tilde{r})_{,r}N_{,r}+2(\log \tilde{r}e^{\nu})_{,r}(B_{23}-L-X)_{,r}-\frac{\mu^2e^{-2\nu}}{\tilde{r}^2}T-B_{02} \\ &-\frac{(\mu^2+2)e^{-2\nu}}{\tilde{r}^2}N-2(\log \tilde{r})_{,r}(\log \tilde{r}e^{2\nu})_{,r}L+2(\phi_{,r})^2L \\ &+2\sigma^2e^{-4\nu}(B_{23}-L-X)-\frac{2Q_e^2e^{-2\nu}}{\tilde{r}^2r^2}\Phi-2\phi_{,r}\Phi_{,r}=0. \end{aligned} \quad (22)$$

Finally, the perturbed equation for the dilaton is obtained by perturbing eq. (3):

$$\begin{aligned} &\frac{1}{\tilde{r}^2}(\tilde{r}^2e^{2\nu}\Phi_{,r})_{,r}+(\sigma^2e^{-2\nu}-\frac{(\mu^2+2)}{\tilde{r}^2}+\frac{2Q_e^2}{\tilde{r}^2r^2})\Phi \\ &+e^{2\nu}(N-3L-2X+2B_{23})_{,r}\phi_{,r}-2\frac{(\tilde{r}^2e^{2\nu}\phi_{,r})_{,r}}{\tilde{r}^2}L+e^{2\nu}B_{02}=0. \end{aligned} \quad (23)$$

The seventh order linear system composed by equations (18)-(23) has been shown to be reducible to three Schrödinger-like equations by using the following procedure. It is well-known that the order of a system of linear differential equations can be reduced, whenever a particular solution of that system is known. A general algorithm for deriving the particular solution which makes the reduction possible as been obtained by Xanthopoulos [14]. Holzhey and Wilczek [13] found that the Xanthopoulos solution one gets from the reduction of the polar equations of Schwarzschild and Reissner-Nordström black holes are *pure gauge* solutions i.e. gauge equivalent to the null perturbation. The general form of the metric (7) has, indeed, a gauge degree of freedom, *i.e.* there exists a one parameter class of coordinate transformations which leaves the form of the metric unchanged. In the case of the GHS black hole the particular *pure gauge* solution which reduces the system (18)-(23) is [13]

$$N^{(0)}=-\sigma^2e^{-\nu}\tilde{r}+e^{4\nu}\nu_{,r}(\tilde{r}e^{-\nu})_{,r}, \quad (24)$$

$$L^{(0)}=(e^{4\nu}(\tilde{r}e^{-\nu})_{,r})_{,r}-e^{4\nu}\nu_{,r}(\tilde{r}e^{-\nu})_{,r}, \quad (25)$$

$$T^{(0)}=e^{4\nu}\tilde{r}^{-1}\tilde{r}_{,r}(\tilde{r}e^{-\nu})_{,r}, \quad (26)$$

$$X^{(0)}=\frac{\mu^2e^{\nu}}{2\tilde{r}}, \quad (27)$$

$$B_{23}^{(0)}=T^{(0)}+L^{(0)}-2\mu^{-2}X^{(0)}, \quad (28)$$

$$\Phi^{(0)}=\phi_{,r}e^{4\nu}(\tilde{r}e^{-\nu})_{,r}. \quad (29)$$

Following Holzhey and Wilczek, we now introduce a new variable S replacing L

$$S=B_{23}-L-X, \quad (30)$$

and make the following substitutions:

$$N=N^{(0)}s+n, \quad B_{23}=B_{23}^{(0)}s+\frac{b}{r\tilde{r}} \quad X=X^{(0)}s+\frac{x}{\tilde{r}}, \quad S=S^{(0)}s, \quad \Phi=\Phi^{(0)}s+\frac{p}{\tilde{r}}. \quad (31)$$

The system is now of order six with respect to the new variables n , x , s , b and p since s does appear through its derivatives only. It is easy to show from Eq. (19) that the first derivative of s can be written as a linear combination of b , x and p as follows

$$s_{,r}=\frac{1}{S^{(0)}}\left(\frac{\tilde{r}_{,r}}{\tilde{r}^2r}b-\frac{\tilde{r}_{,r}}{\tilde{r}^2}x-\frac{\phi_{,r}}{\tilde{r}}p\right). \quad (32)$$

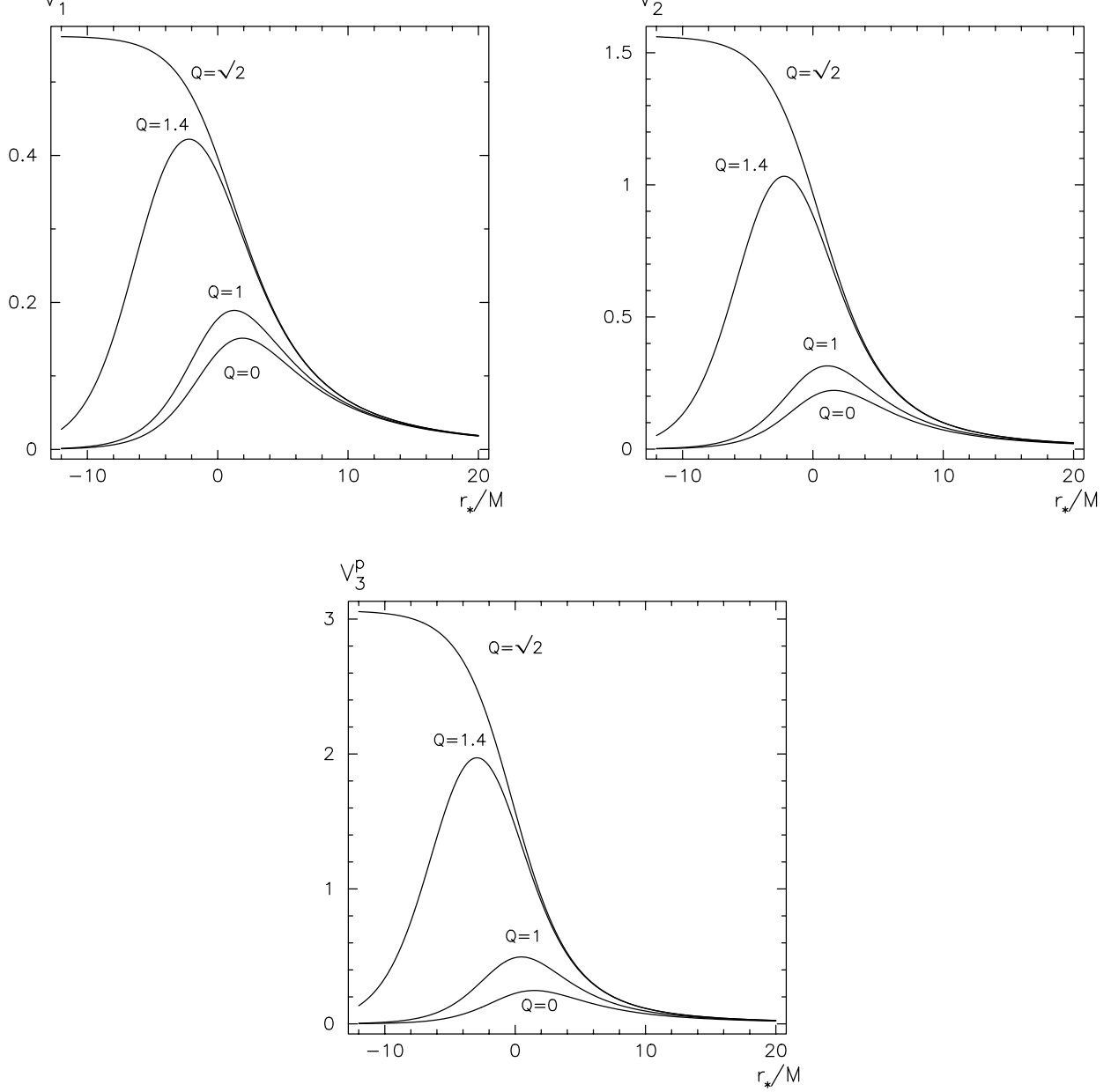


FIG. 2. The $\ell = 2$ polar potentials V_1^p and V_2^p (upper panel) and V_3^p (lower panel) are plotted versus the tortoise coordinate for different values of $Q = Q_e/M$. When the charge is set to zero V_1^a reduces to the Zerilli potential, whereas V_2^p and V_3^p are the potentials of the wave equation describing pure electromagnetic and scalar perturbations on a Schwarzschild background.

Similarly, using (20) and (22), we can eliminate n in favour of x , b , p and their first derivatives. We are now left with only three perturbation variables, x , b and p , governed by three second order equations, namely (21), (18) and (23). In (31), x , b and p have been defined in such a way that their first derivative *with respect to* r_* disappears from the equations they satisfy. Therefore the system has now the desired form

$$\left(\frac{d^2}{dr_*^2} + \sigma^2\right) \mathbf{v} = \mathbf{A} \mathbf{v}, \quad (33)$$

where

$$\mathbf{v} = \begin{pmatrix} x \\ b \\ p \end{pmatrix}, \quad (34)$$

and the components of the symmetric matrix \mathbf{A} are complicated functions of r .

It is convenient to cast \mathbf{A} in the following form:

$$\mathbf{A}(r) = \frac{1}{D(r)} [G(r) \mathbf{T}(r) + P(r) \mathbf{I}], \quad (35)$$

where the polynomials $D(r)$, $G(r)$ and $P(r)$ and the matrix $\mathbf{T}(r)$ are given in the Appendix, and \mathbf{I} is the identity matrix. It is remarkable that the eigenvectors of $\mathbf{T}(r)$ and $\mathbf{A}(r)$ are independent of r . This means that the system can be decoupled with a basis transformation in the x - b - p space. The three eigenvalues are the potentials of three independent Schrödinger equations:

$$\left(\frac{d^2}{dr_*^2} + \sigma^2 \right) Z_i^p = V_i^p Z_i^p \quad (i = 1, 2, 3). \quad (36)$$

It should be noted that for $Q_e = 0$ the equations are already decoupled since the off-diagonal terms of \mathbf{A} vanish (see Appendix) while, as already pointed out, the GHS solution becomes the Schwarzschild solution. In this case, as expected, we find the well-known potentials that rule pure gravitational, electromagnetic, and massless scalar perturbations on a Schwarzschild background, respectively.

Proving the independence of r of the eigenvectors of $\mathbf{T}(r)$ directly, even by means of a symbolic procedure, turns out to be awkward. A straightforward manner is instead to expand the polynomial valued matrix as:

$$\mathbf{T} = \sum_{i=0}^6 r^i \mathbf{T}^{(i)}, \quad (37)$$

where $\mathbf{T}^{(i)}$ are matrices independent of r . It is now very easy to show, for instance with the aid of MATHEMATICA, that the $\mathbf{T}^{(i)}$ commute among themselves, so that they can be diagonalized by the same linear transformation.

The eigenvalue problem for $\mathbf{A}(r)$ is now considerably reduced by means of (35) and (37). In fact, the three potentials can easily be obtained by fixing *first* the values of the parameters M , Q_e and μ , then calculating the eigenvalues of each $\mathbf{T}^{(i)}$, which are now real numbers, and finally summing them up as coefficients of their respective powers of r . The eigenvectors of $\mathbf{A}(r)$ are then obtained straightforwardly by means of (35). The three potentials obtained with the above procedure appear in a rather simple form as functions of r only. This fact turns out to be extremely useful, since to calculate the quasinormal frequencies by means of WKB method one needs up to their sixth derivatives. The potentials V_i^p associated to the wavefunctions Z_i^p (see Eq. 33) are plotted in Fig. 2 for different values of the charge. As in the axial case, when the charge approaches the extremal value, all potentials assume the form of a step. When $Q_e \rightarrow 0$, all off-diagonal components of the matrix \mathbf{A} vanish, and the system of equations (33) decouple into three wave equations for the functions (x, b, p) . From eqs. (31) it is easy to check that, since $B_{23}^{(0)}$ and $\Phi^{(0)}$ vanish, the functions b and Φ become purely electromagnetic and scalar, respectively. Conversely, the variable x is not purely gravitational, since it contains B_{23} . If, however, we explicitly write the function x in terms of B_{23} , X and L in the first Eq. (33), the electromagnetic terms disappear by virtue of the equation satisfied by b , and we are left with the Zerilli equation.

V. THE QUASI-NORMAL MODES

We have computed the complex frequencies of the quasi-normal modes associated to the axial and polar wave equation by using a WKB approximation devised by Schutz and Will [15] and extended to higher orders by Iyer and Will [16]. This approach has been applied to the Schwarzschild [17] and Reissner Nordström [18] cases, and for the fundamental quadrupole mode $l = 2$ agrees with other approaches [19] within 1% both for the real and the imaginary parts of the first 3-4 modes. The agreement improves with increasing angular harmonic and decreasing mode number.

The results of our calculations are shown in table I and II, where we tabulate the real and imaginary part of the frequencies of the first five quasi normal modes associated to the axial and polar potentials, for different values of the harmonic index ℓ , and of the charge Q_e .

The general behaviour of the quasi-normal frequencies for increasing values of the charge is well described in Figure 3. There we plot the real and the imaginary part of the first eigenfrequency of the $\ell = 2$ mode, associated to the potentials V_2^a and V_1^p , as a function of the charge Q_e . It should be reminded that in the limit $Q_e = 0$, these potentials reduce to the Regge-Wheeler and to the Zerilli potentials for the axial and polar gravitational perturbations of a Schwarzschild black hole, respectively. It is well known that the axial and polar perturbations of a Schwarzschild

black hole is a *isospectral*, and this is the reason why, in the limit $Q_e = 0$, the axial (V_2^a) and polar (V_1^p) frequencies shown in Fig. 3 converge to a unique value.

The upper value of Q_e/M we consider in our calculations is $Q_e/M = 1.4$, close to the limiting value $Q_e/M = \sqrt{2}$, where the potential barrier becomes a step which reflects all incident waves.

TABLE I. The frequencies of the first five quasi normal modes associated to the axial and polar wave equations, are written down in units of $1/M$, for $l = 2$ and for increasing values of the charge Q_e .

V_1^a		V_2^a		V_1^p		V_2^p		V_3^p	
Re(σ)	Im(σ)	Re(σ)	Im(σ)	Re(σ)	Im(σ)	Re(σ)	Im(σ)	Re(σ)	Im(σ)
$l = 2 \quad Q_e = 0.2$									
0.374	0.089	0.462	0.095	0.374	0.089	0.457	0.095	0.492	0.097
0.347	0.275	0.441	0.292	0.346	0.275	0.436	0.291	0.472	0.297
0.304	0.472	0.408	0.497	0.302	0.471	0.402	0.496	0.442	0.506
0.249	0.674	0.367	0.708	0.244	0.674	0.360	0.706	0.403	0.719
0.180	0.880	0.317	0.921	0.173	0.880	0.309	0.918	0.358	0.935
$l = 2 \quad Q_e = 0.4$									
0.378	0.090	0.479	0.096	0.377	0.090	0.461	0.095	0.516	0.099
0.351	0.276	0.458	0.295	0.350	0.276	0.440	0.292	0.497	0.301
0.308	0.473	0.427	0.502	0.305	0.473	0.406	0.497	0.468	0.512
0.253	0.676	0.387	0.714	0.248	0.676	0.365	0.707	0.432	0.728
0.185	0.883	0.339	0.929	0.177	0.883	0.315	0.920	0.389	0.945
$l = 2 \quad Q_e = 0.6$									
0.386	0.090	0.508	0.098	0.384	0.090	0.474	0.096	0.552	0.101
0.360	0.279	0.489	0.300	0.356	0.278	0.453	0.294	0.535	0.307
0.318	0.477	0.459	0.510	0.312	0.476	0.421	0.501	0.508	0.521
0.264	0.681	0.422	0.725	0.255	0.680	0.381	0.712	0.476	0.740
0.197	0.889	0.378	0.942	0.184	0.889	0.333	0.926	0.437	0.960
$l = 2 \quad Q_e = 0.8$									
0.401	0.092	0.553	0.101	0.396	0.091	0.500	0.098	0.607	0.104
0.376	0.282	0.536	0.308	0.369	0.281	0.481	0.299	0.592	0.315
0.335	0.483	0.509	0.522	0.325	0.482	0.450	0.508	0.568	0.533
0.283	0.689	0.476	0.741	0.269	0.689	0.413	0.722	0.539	0.756
0.220	0.898	0.437	0.962	0.200	0.899	0.368	0.939	0.506	0.980
$l = 2 \quad Q_e = 1$									
0.429	0.094	0.627	0.105	0.418	0.093	0.545	0.100	0.688	0.107
0.406	0.288	0.612	0.318	0.392	0.286	0.528	0.306	0.675	0.324
0.369	0.492	0.589	0.537	0.350	0.490	0.500	0.520	0.655	0.547
0.322	0.701	0.561	0.762	0.297	0.700	0.466	0.738	0.631	0.775
0.264	0.913	0.529	0.988	0.232	0.913	0.426	0.958	0.603	1.004
$l = 2 \quad Q_e = 1.2$									
0.486	0.097	0.762	0.109	0.466	0.096	0.644	0.105	0.848	0.111
0.468	0.297	0.752	0.330	0.445	0.294	0.631	0.318	0.840	0.336
0.439	0.503	0.736	0.556	0.413	0.502	0.610	0.537	0.826	0.565
0.405	0.715	0.717	0.787	0.375	0.714	0.585	0.761	0.810	0.799
0.365	0.929	0.696	1.019	0.328	0.929	0.556	0.987	0.793	1.034
$l = 2 \quad Q_e = 1.4$									
0.704	0.085	1.252	0.095	0.648	0.083	1.014	0.093	1.403	0.096
0.716	0.258	1.259	0.286	0.666	0.253	1.021	0.280	1.409	0.288
0.744	0.438	1.274	0.480	0.706	0.434	1.038	0.471	1.423	0.483
0.790	0.624	1.297	0.676	0.771	0.624	1.067	0.666	1.444	0.679
0.855	0.816	1.331	0.875	0.863	0.823	1.107	0.865	1.474	0.879

For a Reissner-Nordström black hole the perturbed axial and polar equations can be decoupled in terms of four functions Z_1^\mp and Z_2^\mp , respectively [12]. In the limit $Q_e = 0$, the functions Z_2^\mp reduce to the Regge-Wheeler and to the Zerilli functions, whereas Z_1^\mp reduce to pure axial and polar electromagnetic functions. Moreover, the potentials governing Z_1^- and Z_1^+ are *isospectral*, as well as those for Z_2^- and Z_2^+ . In Figure 4 the same data of Figure 3 are compared with the lowest quasi-normal mode frequency of the functions Z_2^\mp of a Reissner-Nordström black hole. Since the extremal value of the charge for a Reissner-Nordström black hole is $Q_e = 1$, the data stop at that value.

TABLE II. The frequencies of the first five axial and polar quasi normal modes in units $1/M$ are tabulated for $l = 3$ and $l = 4$, for some values of the charge Q_e

V_1^a		V_2^a		V_1^p		V_2^p		V_3^p	
Re(σ)	Im(σ)	Re(σ)	Im(σ)	Re(σ)	Im(σ)	Re(σ)	Im(σ)	Re(σ)	Im(σ)
$l = 3 \quad Q_e = 0.2$									
0.601	0.093	0.664	0.096	0.601	0.093	0.657	0.096	0.687	0.097
0.584	0.282	0.649	0.291	0.584	0.282	0.642	0.290	0.672	0.294
0.555	0.477	0.623	0.492	0.555	0.477	0.616	0.490	0.647	0.497
0.517	0.678	0.590	0.698	0.518	0.678	0.582	0.696	0.615	0.704
0.473	0.882	0.550	0.907	0.473	0.882	0.542	0.904	0.578	0.915
$l = 3 \quad Q_e = .4$									
0.607	0.093	0.686	0.097	0.606	0.093	0.666	0.096	0.716	0.098
0.590	0.283	0.672	0.294	0.589	0.282	0.651	0.291	0.702	0.298
0.562	0.479	0.647	0.496	0.560	0.478	0.625	0.492	0.678	0.503
0.525	0.680	0.614	0.704	0.523	0.680	0.592	0.698	0.648	0.712
0.480	0.885	0.577	0.915	0.479	0.885	0.552	0.908	0.612	0.926
$l = 3 \quad Q_e = .6$									
0.621	0.094	0.724	0.099	0.617	0.094	0.688	0.097	0.762	0.100
0.605	0.285	0.711	0.299	0.601	0.284	0.673	0.294	0.749	0.303
0.576	0.482	0.687	0.504	0.572	0.481	0.648	0.497	0.726	0.511
0.540	0.685	0.657	0.715	0.536	0.684	0.616	0.705	0.698	0.724
0.497	0.891	0.622	0.928	0.492	0.889	0.579	0.916	0.665	0.940
$l = 4 \quad Q_e = 0.2$									
0.811	0.094	0.862	0.096	0.811	0.094	0.854	0.096	0.882	0.097
0.799	0.285	0.851	0.290	0.798	0.285	0.842	0.289	0.870	0.292
0.776	0.479	0.801	0.691	0.776	0.479	0.821	0.487	0.849	0.492
0.746	0.679	0.768	0.898	0.745	0.679	0.792	0.690	0.822	0.696
0.710	0.882	0.729	1.107	0.709	0.882	0.758	0.895	0.789	0.904
$l = 4 \quad Q_e = 0.4$									
0.820	0.095	0.890	0.097	0.818	0.094	0.868	0.096	0.916	0.098
0.808	0.286	0.879	0.293	0.806	0.285	0.856	0.291	0.905	0.296
0.785	0.481	0.858	0.493	0.783	0.481	0.835	0.490	0.885	0.498
0.755	0.681	0.831	0.698	0.753	0.681	0.807	0.693	0.858	0.704
0.720	0.885	0.798	0.906	0.718	0.884	0.774	0.899	0.827	0.913
$l = 4 \quad Q_e = 0.6$									
0.841	0.095	0.936	0.099	0.835	0.095	0.899	0.097	0.969	0.100
0.829	0.288	0.926	0.298	0.823	0.287	0.888	0.294	0.959	0.301
0.807	0.485	0.906	0.501	0.801	0.484	0.867	0.495	0.941	0.506
0.778	0.686	0.881	0.708	0.771	0.685	0.840	0.700	0.916	0.715
0.743	0.891	0.850	0.919	0.736	0.890	0.808	0.908	0.887	0.927

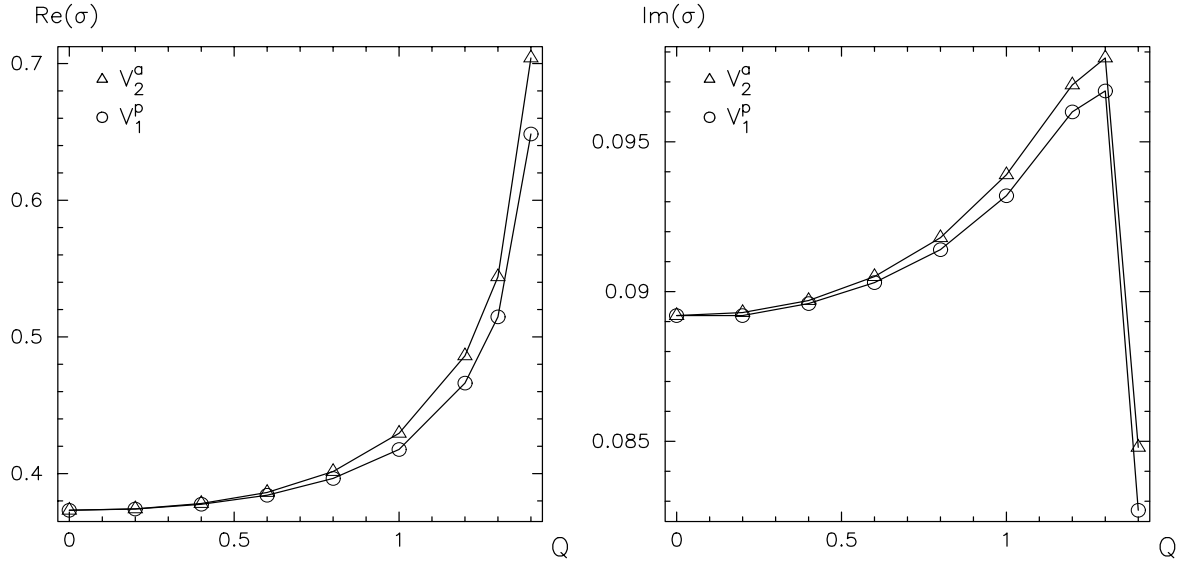


FIG. 3. The real and imaginary part of the frequencies of the quasi-normal modes of the dilaton black holes are plotted versus the electric charge $Q = Q_e/M$, for $\ell = 2$, and for the two potentials which reduce to the Regge-Wheeler and to the Zerilli potentials when the charge is set to zero, i.e. V_2^a (triangles) and V_1^p (circles).

We see that the real part of the frequency increases as a function of the charge both for a dilaton, and for a Reissner-Nordström black hole; similarly, the imaginary part increases and then decreases to a finite value as the charge approaches the limiting value. Since however since the limiting values are different, the imaginary part for Reissner-Nordström begins to decrease while the corresponding GHS values still increase.

Figures 3 and 4 clearly show that the potentials V_2^a and V_1^p of a dilaton black hole *are not isospectral* as they are instead when $Q_e = 0$. In addition, it should be reminded that the potential V_2^a rules the equation for Z_2^a which is a combination of electromagnetic and gravitational perturbations only (cfr. Eq. 13), whereas V_1^p appears in the polar equation for Z_1^p , which is a combination of electromagnetic, gravitational and scalar perturbations.

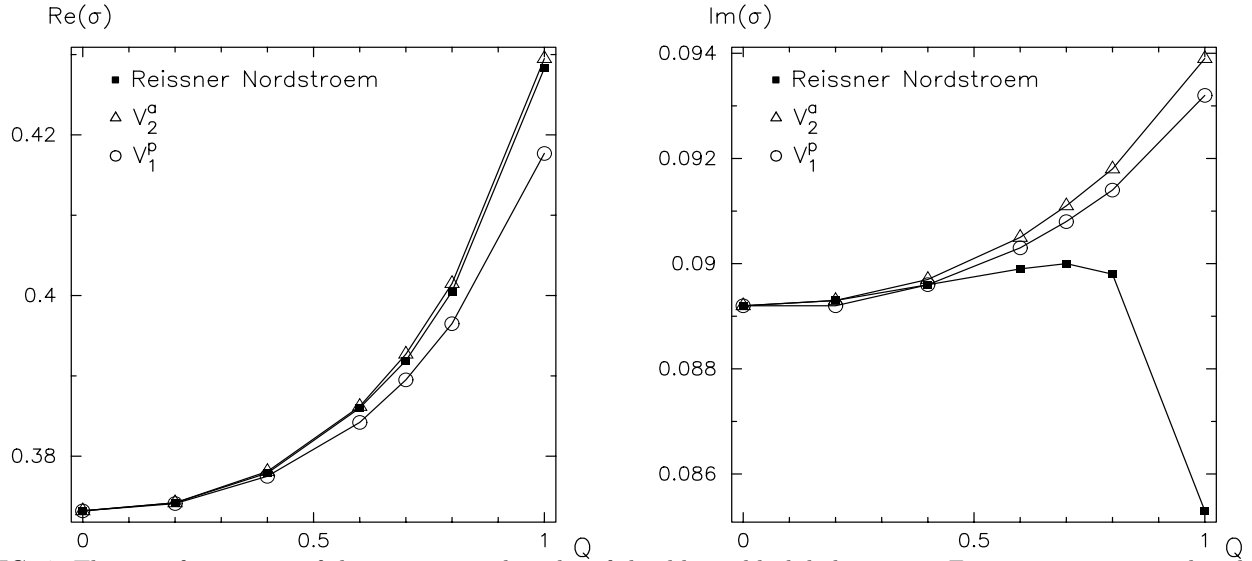


FIG. 4. The eigenfrequencies of the quasi-normal modes of the dilaton black hole given in Figure 3, are compared with those of a Reissner-Nordström black hole for $\ell = 2$. For $Q_e = 0$ both solutions reduce to Schwarzschild and the lines converge to its first, $\ell = 2$, pure gravitational mode $\sigma = 0.373 + 0.089i$. For increasing values of the charge Reissner-Nordström frequencies remain *isospectral*, while GHS frequencies split in two parts, depending on whether they belong to axial or polar modes (see text). Since the extremal value of the charge for a Reissner-Nordström black hole is $Q_e/M = 1$, the data stop at that value.

Finally, in Figure 5 we plot the real and imaginary part of the frequency of the lowest $\ell = 2$ quasi-normal mode for the remaining potentials, V_1^a , V_2^p and V_3^p , as functions of the charge Q_e . When $Q_e = 0$, V_1^a and V_2^p reduce to those governing the pure electromagnetic, axial and polar perturbations of a Schwarzschild black hole, and indeed, they are isospectral in that limit. In the same limit, V_3^p reduces to the potential of the pure scalar perturbations of a Schwarzschild black hole.

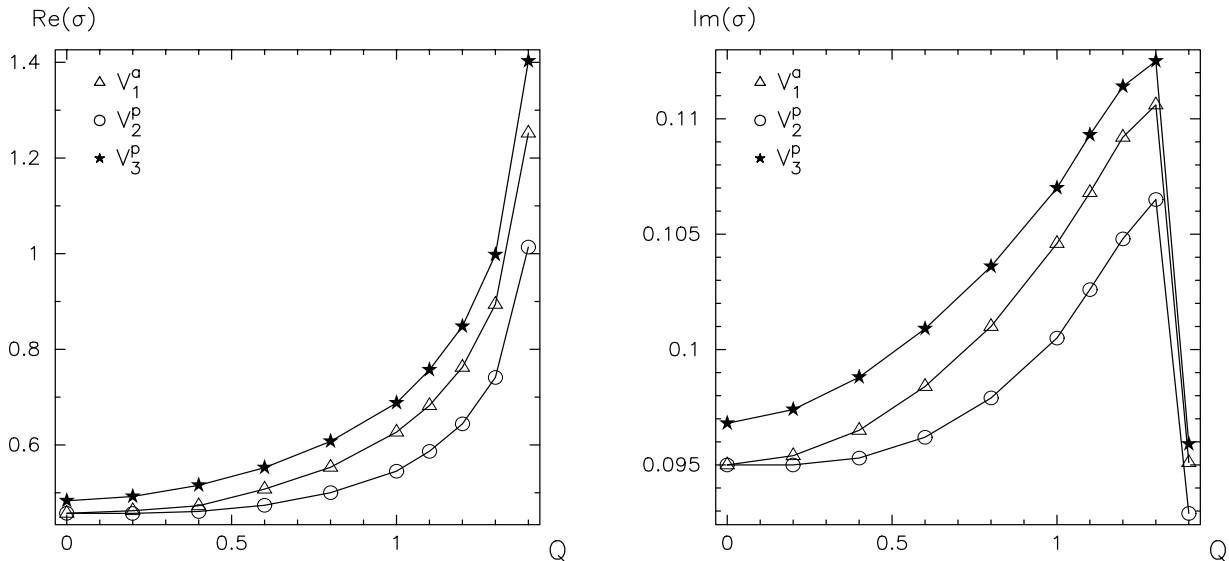


FIG. 5. The real and imaginary part of the frequencies of the lowest $\ell = 2$ -quasi-normal modes of the dilaton black hole, are plotted versus the electric charge $Q = Q_e/M$, for the three potentials V_1^a (triangles), V_2^p (circles) and V_3^p (stars). In the limit $Q = 0$, V_1^a and V_2^p reduce to the potentials governing the axial and polar pure electromagnetic perturbations of a Schwarzschild black hole, whereas V_3^p becomes the potential which appears in the wave equation of the pure scalar perturbations.

VI. CONCLUDING REMARKS

The spectrum of the quasi-normal modes of a charged, dilaton black hole is different from that of a Schwarzschild or a Reissner-Nordström black hole. For a Schwarzschild black hole the perturbations are completely described by the Regge-Wheeler and the Zerilli equations for the axial and the polar perturbations. Although the analytic form of the two potential barriers is different, they are related by a very simple equation (MT, ch. 5, & 43) which allows them to have the same reflexion and trasmission coefficients. Therefore, since the quasi-normal mode frequencies are the singularities of the scattering amplitude, it follows that the two potentials are *isospectral*. Thus, a perturbed Scharzschild black hole emits axial and polar gravitational waves at exactly the same frequencies.

For a Reissner-Nordström black hole the perturbed equations can be reduced to four wave equations, two for the axial and two for the polar perturbations, respectively. The four wave-functions Z_1^\pm and Z_2^\pm , where $+$ stands for polar and $-$ for axial, are a linear combination of the gravitational and the electromagnetic functions belonging to the corresponding parity. It turns out that the two potentials V_1^+ and V_1^- are again related in such a way that they have the same reflection and trasmission coefficients, and the same is true for V_2^\pm . Thus the coupling GW-EM is such that it preveses the isospectrality of the axial and polar perturbations. However there is an important difference with respect to the Schwarzschild case: no quasi-normal mode exists that is purely electromagnetic or gravitational, which means that the excitation of a mode will be accompanied by the simultaneous emission of both gravitational and electromagnetic waves.

For a charged black hole in a theory described by action (1) the situation is different. Let us consider the axial perturbations first. As shown in Section 3, the perturbed equations can be reduced to two wave equations, but the perturbed dilaton does not couple to the electromagnetic and gravitational fields. This is due to the fact that the dilaton is a scalar, and its axial perturbation vanishes. Consequently, the excitation of an axial mode will be accompanied only by the emission of gravitational and electromagnetic waves. However, the dilaton appears in the unperturbed metric functions that determine the shape of the potentials of the axial wave equations. Thus it affects

the scattering properties of the axial potentials. It is interesting to note that the real part of the quasi-normal mode frequencies of the axial potential V_2^a are very similar to those of the Reissner-Nordström black hole (see Fig. 4), even though the dilaton solution does not reduce to the Reissner-Nordström solution in any limiting case.

On the other hand, the two wave equations which describe the polar perturbations of a Reissner-Nordström black hole, are replaced by three wave equations in the case of a dilaton black hole, and they couple the gravitational, electromagnetic and scalar perturbations. This occurrence breaks the symmetry between axial and polar perturbations, and makes the scattering properties of the two parities different (see Fig. 5).

We conclude that for a dilaton black hole the excitation of an axial mode induces the simultaneous emission of gravitational and electromagnetic waves, whereas the excitation of a polar mode is accompanied by the further emission of scalar radiation. In addition, gravitational and electromagnetic polar waves are emitted with frequencies and damping times different from the axial ones.

ACKNOWLEDGMENTS

F.P. wishes to thank Roberto De Pietri, Antonio Scotti and Michele Vallisneri for useful discussions and help in computing technicalities.

VII. APPENDIX

In this Appendix we provide all the elements of the matrix \mathbf{A} that appears in equation (33) and in which are contained all the relevant features of the polar perturbations. It proves convenient to cast \mathbf{A} in the following form

$$\mathbf{A}(r) = \frac{1}{D(r)} [G(r) \mathbf{T}(r) + P(r) \mathbf{I}], \quad (38)$$

where \mathbf{I} is the identity matrix, and $D(r)$, $G(r)$ and $\mathbf{T}(r)$ are:

$$\begin{aligned} D(r) = & 4 \mu Q_e r^4 (-Q_e^2 + M r)^2 \\ & \times (3 M Q_e^4 - 7 M^2 Q_e^2 r - Q_e^4 r + 6 M^3 r^2 - M \mu^2 Q_e^2 r^2 + M^2 \mu^2 r^3) \\ & \times (4 M Q_e^4 - 14 M^2 Q_e^2 r - Q_e^4 r + 12 M^3 r^2 - 2 M \mu^2 Q_e^2 r^2 + 2 M^2 \mu^2 r^3)^2, \end{aligned}$$

$$\begin{aligned} G(r) = & \mu Q_e (2 M - r) r^2 \times (-Q_e^2 + M r) \\ & (3 M Q_e^4 - 7 M^2 Q_e^2 r - Q_e^4 r + 6 M^3 r^2 - M \mu^2 Q_e^2 r^2 + M^2 \mu^2 r^3) / M, \end{aligned}$$

$$\begin{aligned} P(r) = & (1936 M^6 Q_e^6 + 324 M^4 Q_e^8 - 160 M^4 \mu^2 Q_e^8 + 8 M^2 Q_e^{10} + Q_e^{12} - \\ & 2432 M^7 Q_e^4 r - 448 M^5 Q_e^6 r + 624 M^5 \mu^2 Q_e^6 r + 88 M^3 \mu^2 Q_e^8 r + \\ & 2112 M^8 Q_e^2 r^2 - 1136 M^6 Q_e^4 r^2 - 1520 M^6 \mu^2 Q_e^4 r^2 - 64 M^4 Q_e^6 r^2 - \\ & 232 M^4 \mu^2 Q_e^6 r^2 + 24 M^4 \mu^4 Q_e^6 r^2 - 8 M^2 \mu^2 Q_e^8 r^2 - \\ & 1152 M^9 r^3 + 2688 M^7 Q_e^2 r^3 + 1984 M^7 \mu^2 Q_e^2 r^3 - \\ & 272 M^5 \mu^2 Q_e^4 r^3 - 264 M^5 \mu^4 Q_e^4 r^3 + 16 M^3 \mu^2 Q_e^6 r^3 \\ & - 4 M^3 \mu^4 Q_e^6 r^3 - 1152 M^8 r^4 - 960 M^8 \mu^2 r^4 + 832 M^6 \mu^2 Q_e^2 r^4 + \\ & 464 M^6 \mu^4 Q_e^2 r^4 - 16 M^4 \mu^2 Q_e^4 r^4 - 28 M^4 \mu^4 Q_e^4 r^4 - \\ & 16 M^4 \mu^6 Q_e^4 r^4 - 384 M^7 \mu^2 r^5 - 224 M^7 \mu^4 r^5 + 64 M^5 \mu^4 Q_e^2 r^5 + \\ & 32 M^5 \mu^6 Q_e^2 r^5 - 32 M^6 \mu^4 r^6 - 16 M^6 \mu^6 r^6) / 8 M^2 \mu Q_e. \end{aligned}$$

$$\begin{aligned} \mathbf{T}_{11} = & 2448 M^6 Q_e^6 + 324 M^4 Q_e^8 - 160 M^4 \mu^2 Q_e^8 + 8 M^2 Q_e^{10} + Q_e^{12} + 8 M^3 Q_e^4 \\ & (-496 M^4 - 64 M^2 Q_e^2 + 110 M^2 \mu^2 Q_e^2 - 4 Q_e^4 + 11 \mu^2 Q_e^4) r + 8 M^2 Q_e^2 \\ & (408 M^6 + 42 M^4 Q_e^2 - 222 M^4 \mu^2 Q_e^2 - 45 M^2 \mu^2 Q_e^4 + 3 M^2 \mu^4 Q_e^4 - \\ & \mu^2 Q_e^6) r^2 + 4 M^3 (-288 M^6 + 400 M^4 \mu^2 Q_e^2 + 108 M^2 \mu^2 Q_e^4 - \\ & 34 M^2 \mu^4 Q_e^4 + 4 \mu^2 Q_e^6 - \mu^4 Q_e^6) r^3 + 4 M^4 \mu^2 (-144 M^4 - \end{aligned}$$

$$32 M^2 Q_e^2 + 52 M^2 \mu^2 Q_e^2 - 4 Q_e^4 - 7 \mu^2 Q_e^4 - 4 \mu^4 Q_e^4) r^4 + \\ 32 M^5 \mu^4 (-3 M^2 + 2 Q_e^2 + \mu^2 Q_e^2) r^5 - 16 M^6 \mu^4 (2 + \mu^2) r^6$$

$$\mathbf{T}_{21} = 128 M^5 \mu Q_e^7 + 8 M^2 \mu Q_e^5 (-76 M^4 + 8 M^2 \mu^2 Q_e^2 - \\ Q_e^4) r + 16 M^3 \mu Q_e^3 (56 M^4 + 22 M^2 Q_e^2 - 8 M^2 \mu^2 Q_e^2 + Q_e^4 - \\ 2 \mu^2 Q_e^4) r^2 + 32 M^4 \mu Q_e (-12 M^4 - 24 M^2 Q_e^2 + \\ 2 M^2 \mu^2 Q_e^2 + 6 \mu^2 Q_e^4 + \mu^4 Q_e^4) r^3 + 32 M^5 \mu Q_e \\ (12 M^2 - 9 \mu^2 Q_e^2 - 2 \mu^4 Q_e^2) r^4 + 32 M^6 \mu^3 (4 + \mu^2) Q_e r^5$$

$$\mathbf{T}_{31} = 16 M^3 \mu \sqrt{2 + \mu^2} Q_e^2 r (Q_e^2 - M r) (14 M^2 Q_e^2 - Q_e^4 - \\ 24 M^3 r + 4 M \mu^2 Q_e^2 r + 6 M^2 r^2 - 6 M^2 \mu^2 r^2 - \mu^2 Q_e^2 r^2 + 2 M \mu^2 r^3)$$

$$\mathbf{T}_{22} = 2064 M^6 Q_e^6 + 260 M^4 Q_e^8 - 160 M^4 \mu^2 Q_e^8 + 8 M^2 Q_e^{10} + Q_e^{12} + \\ 4 M Q_e^4 (-536 M^6 - 164 M^4 Q_e^2 + 116 M^4 \mu^2 Q_e^2 + \\ 6 M^2 Q_e^4 + 18 M^2 \mu^2 Q_e^4 + Q_e^6) r + 8 M^2 Q_e^2 \\ (72 M^6 + 6 M^4 Q_e^2 - 98 M^4 \mu^2 Q_e^2 - 32 M^2 Q_e^4 - \\ 43 M^2 \mu^2 Q_e^4 - 5 M^2 \mu^4 Q_e^4 - Q_e^6 + \mu^2 Q_e^6) r^2 + \\ 4 M^3 Q_e^2 (432 M^4 + 256 M^4 \mu^2 + 48 M^2 Q_e^2 + \\ 12 M^2 \mu^2 Q_e^2 - 18 M^2 \mu^4 Q_e^2 - 12 \mu^2 Q_e^4 - \\ \mu^4 Q_e^4) r^3 + 4 M^4 (-288 M^4 - 144 M^4 \mu^2 + 160 M^2 \mu^2 Q_e^2 + \\ 76 M^2 \mu^4 Q_e^2 + 8 \mu^2 Q_e^4 - 11 \mu^4 Q_e^4 - \\ 4 \mu^6 Q_e^4) r^4 + 16 M^5 \mu^2 (-24 M^2 - 12 M^2 \mu^2 + 5 \mu^2 Q_e^2 + \\ 2 \mu^4 Q_e^2) r^5 - 16 M^6 \mu^4 (2 + \mu^2) r^6$$

$$\mathbf{T}_{32} = 8 M^2 \sqrt{2 + \mu^2} Q_e (-16 M^3 Q_e^6 - 36 M^4 Q_e^4 r + \\ 8 M^2 Q_e^6 r - 8 M^2 \mu^2 Q_e^6 r + Q_e^8 r + 192 M^5 Q_e^2 r^2 - \\ 52 M^3 Q_e^4 r^2 - 16 M^3 \mu^2 Q_e^4 r^2 - 2 M Q_e^6 r^2 + \\ 4 M \mu^2 Q_e^6 r^2 - 144 M^6 r^3 + 48 M^4 Q_e^2 r^3 + 72 M^4 \mu^2 Q_e^2 r^3 - \\ 16 M^2 \mu^2 Q_e^4 r^3 - 4 M^2 \mu^4 Q_e^4 r^3 - 48 M^5 \mu^2 r^4 + \\ 12 M^3 \mu^2 Q_e^2 r^4 + 8 M^3 \mu^4 Q_e^2 r^4 - 4 M^4 \mu^4 r^5)$$

$$\mathbf{T}_{33} = 1936 M^6 Q_e^6 + 324 M^4 Q_e^8 - 160 M^4 \mu^2 Q_e^8 + 8 M^2 Q_e^{10} + Q_e^{12} + \\ 8 M^3 Q_e^4 (-304 M^4 - 56 M^2 Q_e^2 + 78 M^2 \mu^2 Q_e^2 + \\ 11 \mu^2 Q_e^4) r + 8 M^2 Q_e^2 (264 M^6 - 142 M^4 Q_e^2 - \\ 190 M^4 \mu^2 Q_e^2 - 8 M^2 Q_e^4 - 29 M^2 \mu^2 Q_e^4 + \\ 3 M^2 \mu^4 Q_e^4 - \mu^2 Q_e^6) r^2 + 4 M^3 (-288 M^6 + 672 M^4 Q_e^2 + \\ 496 M^4 \mu^2 Q_e^2 - 68 M^2 \mu^2 Q_e^4 - 66 M^2 \mu^4 Q_e^4 + \\ 4 \mu^2 Q_e^6 - \mu^4 Q_e^6) r^3 + 4 M^4 (-288 M^4 - 240 M^4 \mu^2 + \\ 208 M^2 \mu^2 Q_e^2 + 116 M^2 \mu^4 Q_e^2 - 4 \mu^2 Q_e^4 - \\ 7 \mu^4 Q_e^4 - 4 \mu^6 Q_e^4) r^4 + 32 M^5 \mu^2 (-12 M^2 - \\ 7 M^2 \mu^2 + 2 \mu^2 Q_e^2 + \mu^4 Q_e^2) r^5 - 16 M^6 \mu^4 (2 + \mu^2) r^6$$

- [1] D. Garfinkle, G. T. Horowitz and A. Strominger *Phys. Rev.* **D43** 3140 (1990)
[2] G. Veneziano, *Phys. Lett.* **B265** (1991) 287.

- [3] M. Maggiore, gr-qc/9909001
- [4] See M. Brunetti, E. Coccia, V. Fafone and F. Fucito, *Phys. Rev.* **D59** 044027 (1999) and references therein.
- [5] M. Maggiore and A. Nicolis, gr-qc/9907055
- [6] K.D. Kokkotas and B. G. Schmidt, *Living Reviews in Relativity*, gr-qc/9909058
- [7] J. D. Bekenstein *Phys. Rev.* **D5** 1239 (1972)
- [8] J. D. Bekenstein *Ann. Phys.* **82** 535 (1973)
- [9] K. A. Bronnikov and Y. N. Kireyev *Phys. Lett.* **A 67** 95 (1978)
- [10] V. Ferrari and B. C. Xantopoulos *Phys. Rev.* **D41** 3652 (1990)
- [11] G. W. Gibbons and K. Maeda *Nuc. Phys.* **B 298** 741 (1988)
- [12] S. Chandrasekhar, *The Mathematical Theory of Black Holes* Oxford Science Publication, 1983.
- [13] C. F. E. Holzhey and F. Wilczek *Nuc. Phys.* **B380** 447 (1992)
- [14] B. C. Xantopoulos *Proc. Roy. Soc. (London)* **A378** 61 (1981)
- [15] B. F. Schutz and C. M. Will *Astrophys. J. Lett.* **291**
- [16] S. Iyer and C. M. Will *Phys. Rev.* **D 35** 3621 (1987)
- [17] S. Iyer *Phys. Rev.* **D 35** 3632 (1986)
- [18] K. D. Kokkotas and B. F. Schutz *Phys. Rev.* **D 37** 3378 (1988)
- [19] The pioneer numerical work for Schwarzschild is that of S. Chandrasekhar and S. Detweiler, *Proc. R. Soc. (London)* **A 344** 441 (1975), extended to Reissner Nordström by D. L. Gunter *Phyl. Trans. Roy. Soc. (London)* **299** 497 (1980). Higher modes are obtained with great precision with the semi-analytical method developed in E. W. Leaver *Proc. R. Soc.* **A 402** 285 (1985) and there applied to Schwarzschild and Kerr black holes. A more extended bibliography can be found in Ref. [6].